ELSEVIER

S0032-3861(96)00261-3

Polymer Vol. 37 No. 19, pp. 4425–4429, 1996

0032-3861/96/$15.00 + 0.00

Crystallization of nanoscale-confined diblock copolymer chains

Ian W. Hamley
School of Chemistry, University of Leeds, Leeds, West Yorkshire LS2 9JT, UK

and J. Patrick A. Fairclough and Anthony J. Ryan*
Manchester Materials Science Centre, UMIST, Grosvenor Street, Manchester M1 7HS, UK

and Frank S. Bates
Department of Chemical Engineering and Materials Science, University of Minnesota, Minneapolis, MN 55455, USA

and Elizabeth Towns-Andrews
CLRC Daresbury Laboratory, Warrington WA4 4AD, UK
(Received 9 February 1996)

Crystallization of polymer chains between hard glassy walls or between amorphous domains in a nanoscale lamellar structure has been observed using simultaneous small-angle and wide-angle X-ray scattering (SAXS/WAXS). Semicrystalline symmetric diblock copolymers containing poly(ethylene) (PE) and a room-temperature glassy or amorphous component were shear oriented in the high temperature lamellar melt, then quenched below the PE melt temperature. For the glassy sample, the orientation of chain-folded PE stems was deduced from SAXS/WAXS peak positions to be parallel to the lamellar interface. Diffuse scattering bars consistent with lateral positional correlations of the PE crystallites were observed only in the SAXS patterns for the glassy sample with the X-rays incident parallel to the lamellae. In contrast, in a sample containing amorphous lamellae, PE crystallization occurred with weak crystallite orientation and no lateral positional correlations of crystallites. Copyright © 1996 Elsevier Science Ltd.

(Keywords: block copolymer; crystallization; X-ray diffraction; modelling)

Introduction

Block copolymers are remarkable self-assembling systems that can order with amorphous, glassy or crystalline components[1]. In the melt of a diblock copolymer, where both polymer chains are amorphous, a number of ordered structures are stable below the order–disorder transition (ODT), depending on the composition of the copolymer specified by the volume fraction of one component, f, the degree of polymerization, N, and the temperature which is contained in the Flory–Huggins interaction parameter $\chi = A/T + B$, where A and B are system-dependent constants[2]. The lamellar, hexagonal-packed cylinder and body-centred cubic micelle structures that are accounted for by the simplest mean-field theory[3] have recently been supplemented by the observation of complex layered[4] and bicontinuous cubic[5,6] structures that have been observed near the ODT in the phase diagram between lamellae and hexagonal-packed cylinders.

The presence of a component that can crystallize or vitrify leads to the possibility of preparing structures such as solid spheres dispersed in a rubbery or amorphous matrix[7]. However, crystallization in semicrystalline diblocks quenched from the homogeneous melt or the lamellar or hexagonal-packed cylinder microphase-separated melt overwhelms microphase separation at temperatures below the crystalline component melt temperature, T_m[8,9]. The solvent casting process may play an important role in trapping non-equilibrium structures such as crystalline spheres in a rubbery matrix because the crystallizable block can precipitate from solution in a non-selective solvent[10].

We have previously investigated crystallization in a series of monodisperse diblock copolymers of poly(ethylene)–poly(ethylethylene) (PE–PEE) and poly(ethylene)–poly(ethylene–propylene) (PE–PEP). Using SAXS, WAXS and differential scanning calorimetry (d.s.c.) we found that, irrespective of the melt structure, a lamellar structure containing semicrystalline PE was formed below $T_m \simeq 106°C$, with PE crystallizing in its usual orthorhombic form. The PE degree of crystallinity was found to be $(40 \pm 10)\%$ and the kinetics were shown to obey an Avrami-type equation consistent with nucleation and growth of lamellar spherulites[8].

The orientation of crystallized polymer chains in semicrystalline diblock copolymers has been investigated previously, with conflicting results. Chain folding of poly(ethylene oxide) perpendicular to the lamellar interface was inferred for poly(ethylene oxide)–poly(isoprene) diblocks studied using microscopy and X-ray diffraction[11]. However, Douzinas and Cohen found that poly(ethylene-*co*-butylene) folds parallel to the interface in crystallized poly(ethylene-*co*-butylene)–poly(ethylethylene) diblocks, from a pole figure analysis of WAXS data for oriented samples[12].

* To whom correspondence should be addressed

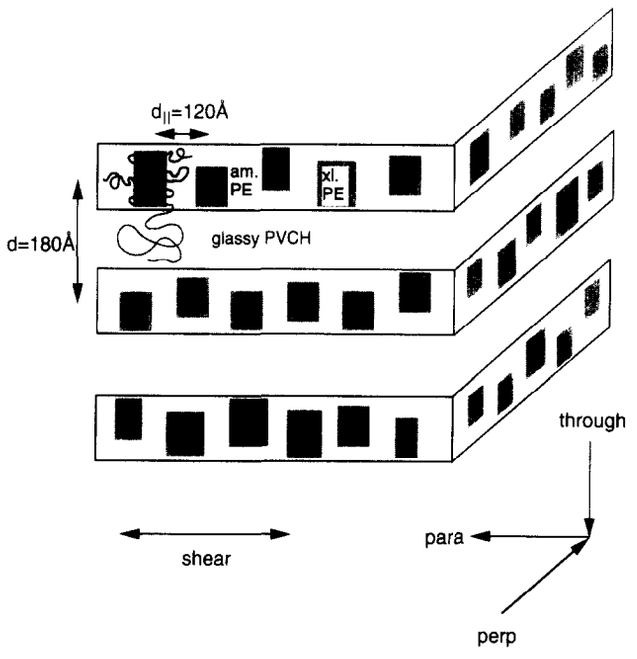

Figure 1 A qualitative model for the lamellar organization in the semicrystalline PE–PVCH sample. The PE domain consists of amorphous and crystalline regions, with a preferred inter-crystallite separation as shown by the Markov model (*Figure 4*). The convention used to label the scattering patterns is also shown

We have studied crystallization in diblock copolymers containing poly(ethylene) and poly(ethylene–propylene) (PEP, glass transition temperature, $T_g \simeq -56°C$) or poly(vinyl cyclohexane) (PVCH, $T_g \simeq 140°C$). Samples were oriented using reciprocating shear in a home-made device[13] and then cooled to room temperature, where PVCH is glassy and PEP is rubbery. The samples were then cut up in three orthogonal planes, one of which is the shear plane. The convention for labelling samples by the orientation of the X-ray beam with respect to the lamellar planes and the shear direction is shown in *Figure 1*. By performing simultaneous SAXS and WAXS experiments we deduce the PE stem orientation in a lamellar system with a nanoscale lamellar thickness with either alternating semicrystalline and glassy domains or alternating semicrystalline and rubbery domains. We are not aware of previous studies on crystallization in semicrystalline–glassy diblocks.

A remarkable feature of the SAXS data for the perpendicular orientation of the PE–PVCH sample that is not observed for the PE–PEP sample is the observation of a type of diffuse scatter that appears to be due to two-dimensional crystal growth, with weak inter-crystallite correlations.

Experimental

The PE–PEP copolymer was synthesized by anionic polymerization of a poly(diene) precursor, followed by catalytic hydrogenation[14], while the PE–PVCH sample was prepared by hydrogenation of a monodisperse poly(1,4-butadiene)–poly(styrene) precursor[15]. Anionic polymerization ensures a low polydispersity index ($M_w/M_n < 1.1$). The PE–PEP sample has a PE volume fraction $f_{PE} = 0.50$ and a molecular weight $M_n = 128\,000$. The corresponding values for the PE–PVCH sample are $f_{PE} = 0.52$ and $M_n = 15\,000$. The crystallization of a range of symmetric and asymmetric poly(ethylene)-containing diblock copolymers will be discussed more fully elsewhere[16].

The SAXS/WAXS experiments were performed on station 16.1 at the Synchrotron Radiation Source, Daresbury Laboratory, UK. This is a fixed wavelength ($\lambda = 1.4$ Å) high-intensity diffraction station optimized for low angle measurements[17]. The incident beam is defined by five horizontal and five vertical slits. Vertical focusing was provided by a bent mirror with the X-ray source focused at the SAXS detector, while monochromatization was achieved using a Ge(111) bent triangular crystal, which also provides horizontal focusing. The SAXS data were acquired using either a two-dimensional multiwire gas detector with 512 × 512 pixels or an image plate. WAXS patterns were recorded on an image plate with a central hole drilled through it to allow the passage of the X-rays to the SAXS detector. The SAXS data were corrected for detector response and background scattering and the q ($= 4\pi \sin\theta/\lambda$) (where 2θ is the scattering angle) scale was calibrated with a sample of wet collagen (rat-tail) which gives multiple orders of Bragg peaks with a period of 670 Å.

Results

X-ray patterns for the PE–PVCH sample are shown in *Figure 2*. The WAXS data for the perpendicular orientation clearly show the PE unit cell orientation. The inner diffuse ring of scattering is from amorphous PE, and superimposed on this are four (110) reflections at an angle $\phi \simeq 53°$ with respect to the horizontal axis and two equatorial (200) type peaks. The angle ϕ is close to the value expected ($\phi = 56°$) for the projection along the c axis of the diffraction pattern of the body-centred orthorhombic PE unit cell[18]. The peak q values are close to those observed for the homopolymer, showing that the crystal structure is not substantially distorted when crystallization occurs between glassy walls in the solidified block copolymer.

The presence of three orders of reflection along the equator in the SAXS data for the perpendicular orientation indicates that the solid structure is lamellar, with a period $\simeq 180$ Å. Thus PE has crystallized between glassy walls with a separation on this lengthscale. Also apparent in the SAXS data are two broad bars of diffuse scatter, centred on the meridian and parallel to the equator. This diffuse scatter indicates that crystallization has not occurred randomly, but rather with a preferred orientation and a characteristic in-plane lengthscale. A model for the diffuse scatter is discussed shortly.

Because the (200) reflections in the WAXS pattern lie along the same direction as the Bragg peaks in the SAXS pattern, taken concurrently, we can deduce the orientation of the chain-folded PE stems with respect to the layer normal. Because the stems lie along the c axis of the unit cell[12] (see *Figure 1*), they must be perpendicular to both the shear direction and the layer normal in this orientation. For the parallel orientation of this sample the SAXS pattern also contains at least three equally spaced orders of reflection. However, these reflections are smeared into broad arcs, consistent with a much lower degree of lamellar orientational order for the parallel orientation. This is not surprising because the lamellar order is expected to be less perfect in a plane

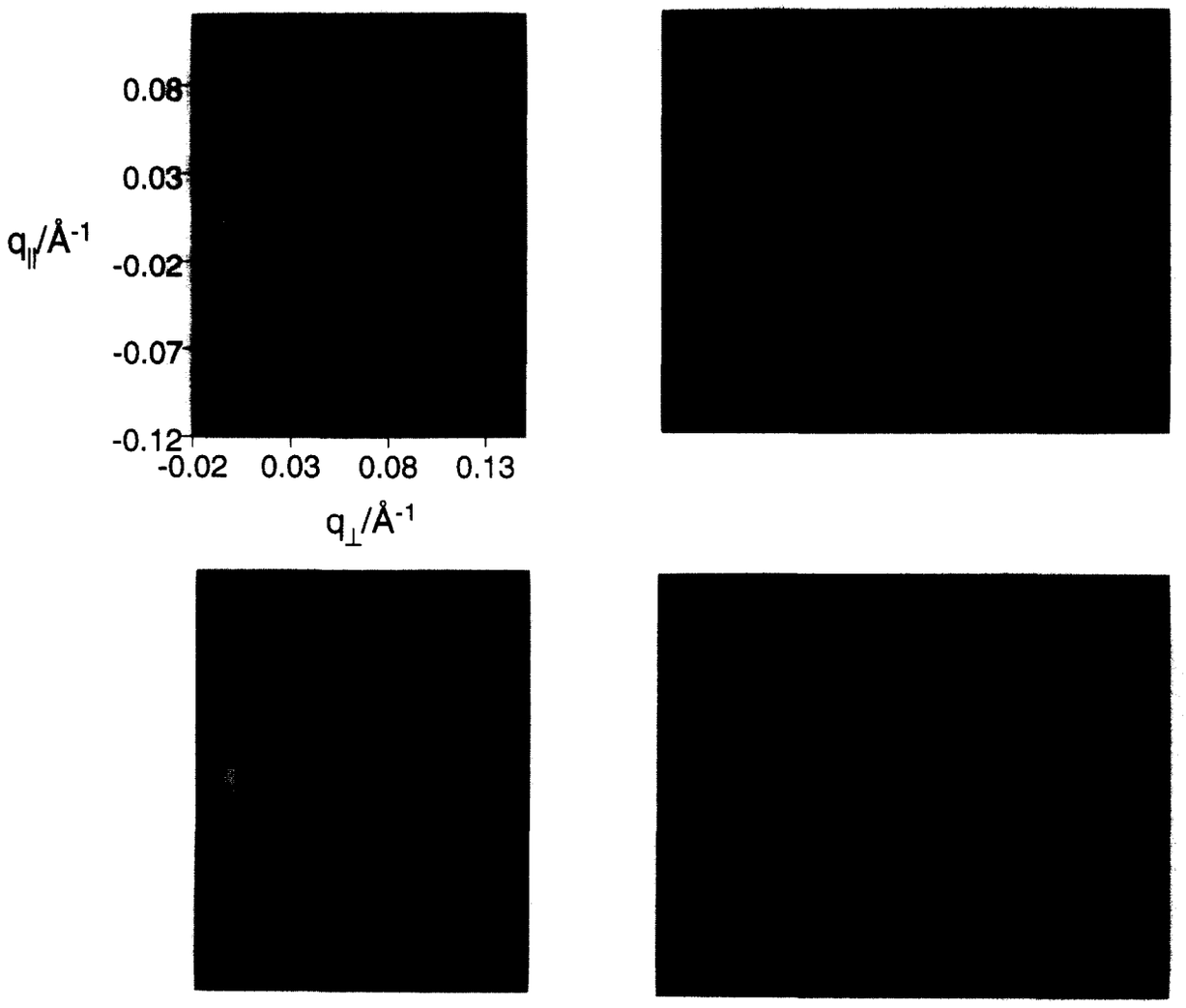

Figure 2 X-ray diffraction patterns from PE–PVCH for different orientations with respect to the shear direction and lamellar stacks. Left: WAXS, right: SAXS; top: perpendicular orientation, bottom: parallel orientation

normal to the shear direction[14]. The (110) and (200) reflections in the WAXS pattern are noticeably less well oriented than for the perpendicular orientation, showing that the unit cells are less well oriented. We were unable to obtain monodomain scattering patterns for the sample in the through orientation because of difficulties in cutting the glassy sample.

There are no diffuse scattering bars in the SAXS patterns for PE–PEP-3. The data for the perpendicular orientation at room temperature in *Figure 3* show three orders of Bragg reflections, consistent with a lamellar structure, but the absence of diffuse scattering bars shows that there is no regular in-plane positional order of crystallites. The weak ring of diffuse scattering from semicrystalline PE centred at $q \simeq 0.045$ Å^{-1} is not visible on this scale. The WAXS patterns for the perpendicular orientation shown in *Figure 3* are consistent with a weak preferred unit cell orientation. Thus, in contrast to the sample containing glassy PVCH, crystallization in a diblock with amorphous PEP domains has occurred with an irregular distribution of crystallite positions, but with cell orientational order of the c axis of the unit cell.

Discussion

We have modelled the diffuse scatter in the SAXS pattern for PE–PVCH using a Markov model for a one-dimensional lattice[19]. This is equivalent to a one-dimensional Ising model with nearest-neighbour pair interactions[20]. Markov models have previously been used to describe the kinetics of growth of lamellar crystals formed by chain-folding polymers[21], but we are unaware of its application to describe diffuse scattering from semicrystalline polymers. In the Markov model, the probability of a site crystallizing ($A_{j,k} = 1$ if the site is crystalline, $A_{j,k} = 0$ otherwise) depends only on the occupancy of the previous site in that layer. In particular, the probability for crystallite occupancy at site j is given by

$$P(x_{j,k} = 1/A_{j-1,k}) = \alpha + \beta A_{j-1,k} \qquad (1)$$

where α and β are the probabilities that a site is crystalline given that the previous one is not or is crystalline, respectively.

A model with $\alpha = 0.8$ and $\beta = -0.6$ best describes our data in terms of the width of the diffuse scattering bars, and the overall fraction of sites occupied by crystallites is $\phi = 0.5$, close to the determined degree of crystallinity. An example of a stack of one-dimensional Markov lattices generated using this model is shown in *Figure 4*. Consistent with the location of the diffuse scattering bars

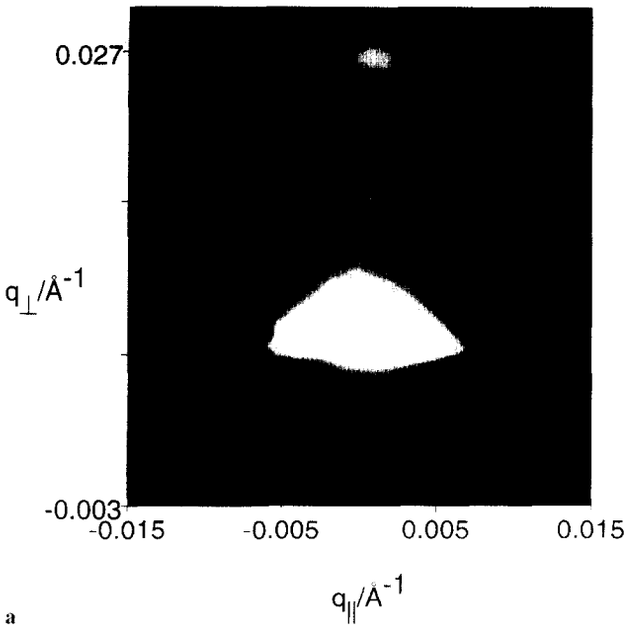

a

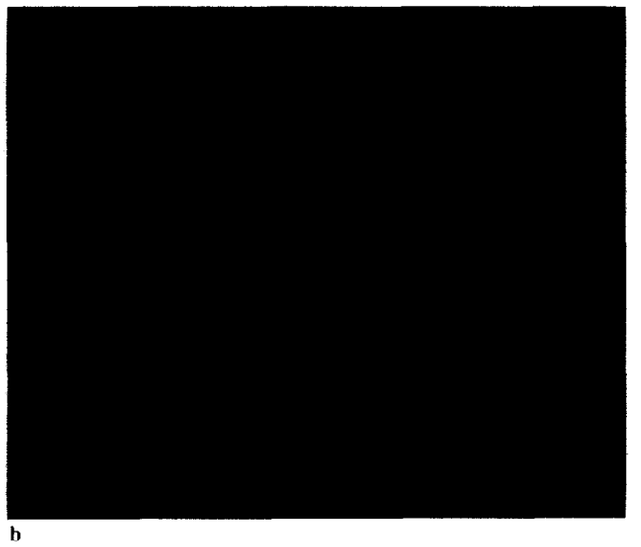

b

Figure 3 X-ray diffraction patterns from PE–PEP-3 in the perpendicular orientation. (a) SAXS data; (b) WAXS data. The first order reflection in the SAXS data has been overexposed to highlight the higher orders

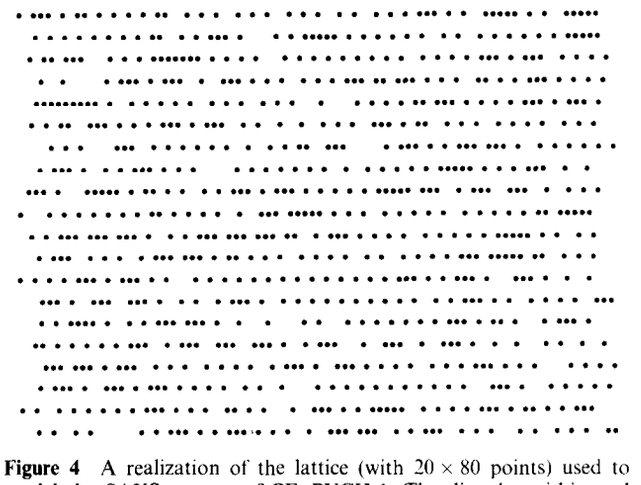

Figure 4 A realization of the lattice (with 20×80 points) used to model the SAXS pattern of PE–PVCH-1. The disorder within and between stacks of linear arrangements of crystallites (represented as points) leads to diffuse scattering

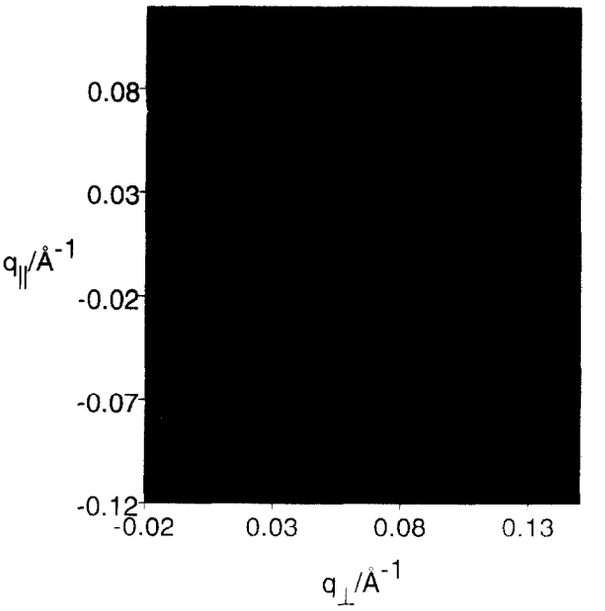

Figure 5 The scattering pattern computed for the model based on stacked Markov chains

with respect to the Bragg reflections we use an in-plane repeat $d_\parallel = 0.35d$, where d is the layer period. Using an enlarged ($N = 300$) version of this model, the scattered intensity is computed as

$$I(q_x, q_y) = \sum_{j=1}^{N}\sum_{k=1}^{N}\sum_{l=1}^{N}\sum_{m=1}^{N} A_{j,k}A_{l,m} \times \exp[i(q_x X_{jl} + q_y Y_{km})] \quad (2)$$

Here $X_{jl} = x_j - x_l$ and $Y_{km} = y_k - y_m$, with $x_j = jd_x$ etc., define inter-site vectors. The calculated scattering pattern (*Figure 5*) may be compared to the SAXS data for the PE–PVCH sample in the perpendicular orientation (*Figure 2*). The intensity is reduced at large q due to the inclusion in the model of a Debye–Waller factor, $\exp[-\sigma^2 q_x^2]$ with $\sigma^2 = 0.015$, that accounts for lattice disorder. Because we are not able to calculate a crystallite form factor, the Debye–Waller factor also simulates the effect of the reduction in intensity due to the form factor. The main features of the SAXS pattern are clearly reproduced in the model, especially the location and width of the diffuse scattering bar. We have not attempted to allow for the orientational disorder of the lamellar stacks in our model, which is simply intended to account for the presence of diffuse scattering bars. The diffuse scattering intensity from a one-dimensional Markov lattice is given by[19]

$$I(q)_{\text{diffuse}} = K(1-\beta^2)[1+\beta^2-2\beta\cos(qd)]^{-1} \quad (3)$$

where K is a constant and d is the period. We have verified that this model fits a cross-section through the diffuse scattering in the SAXS data for PE–PVCH with $\beta = -0.64$, determined in a least-squares fit.

In summary, we have determined how poly(ethylene) crystallizes in nanoscale confinement by performing X-ray scattering experiments on shear-oriented diblock copolymers containing either a glassy or an amorphous block where the poly(ethylene) crystallizes in a lamellar structure. By comparing the location of SAXS peaks

from lamellae and WAXS peaks from the crystal unit cell, poly(ethylene) was shown to chain-fold with stems parallel to the lamellae in a sample containing glassy PVCH. Furthermore, the crystallite positions in this sample are laterally correlated in the plane of the shear gradient, as is shown by meridional diffuse scatter bars in the corresponding SAXS pattern. A simple lattice model well describes this diffuse scatter. For a sample containing amorphous PEP, on the other hand, poly(ethylene) crystallization occurred with no lateral positional correlations.

Acknowledgement

This work was supported by the award of a grant from the Engineering and Physical Sciences Research Council, UK, to A.J.R. and I.W.H.

References

1 Goodman, I. (Ed.) 'Developments in Block Copolymers', Vol. 1, Applied Science, New York, 1982; Vol. 2, Applied Science, New York, 1985
2 Bates, F. S. and Fredrickson, G. H. *Annu. Rev. Phys. Chem.* 1990, **41**, 525
3 Leibler, L. *Macromolecules* 1980, **13**, 1602
4 Hamley, I. W., Gehlsen, M. D., Khandpur, A. K., Koppi, K. A., Rosedale, J. H., Schulz, M. F., Bates, F. S., Almdal, K. and Mortensen, K. *J. Phys. France II* 1994, **4**, 2161
5 Hajduk, D. A., Harper, P. E., Gruner, S. M., Honeker, C. C., Kim, G., Thomas, E. L. and Fetters, L. J. *Macromolecules* 1994, **27**, 4063
6 Förster, S., Khandpur, A. K., Zhao, J., Bates, F. S., Hamley, I. W., Ryan, A. J. and Bras, W. *Macromolecules* 1994, **27**, 6922
7 Folkes, M. J. and Keller, A. in 'The Physics of Glassy Polymers' (Ed. R. N. Howard), Applied Science, London, 1973
8 Ryan, A. J., Hamley, I. W., Bras, W. and Bates, F. S. *Macromolecules* 1995, **28**, 3680
9 Rangarajan, R., Register, R. A. and Fetters, L. J. *Macromolecules* 1993, **26**, 4640
10 Veith, C. A., Cohen, R. E. and Argon, A. S. *Polymer* 1991, **32**, 1545
11 Hirata, E., Ijitsu, T., Soen, T., Hashimoto, T. and Kawai, H. *Polymer* 1975, **16**, 249
12 Douzinas, K. C. and Cohen, R. E. *Macromolecules* 1992, **25**, 5030
13 Koppi, K. A., Tirrell, M., Bates, F. S., Almdal, K. and Mortensen, K. *J. Rheol.* 1994, **38**, 999
14 Rosedale, J. H., Bates, F. S., Almdal, K., Mortensen, K. and Wignall, G. D. *Macromolecules* 1995, **28**, 1429
15 Gehlsen, M. D. and Bates, F. S. *Macromolecules* 1993, **26**, 4122
16 Hamley, I. W., Fairclough, J. P. A., Ryan, A. J., Terrill, N.J., Lipic, P., Bates, F. S. and Towns-Andrews, E. *Macromolecules* in press
17 Bliss, N., Bordas, J., Fell, B. D., Harris, N. W., Helsby, W. I., Mant, G. R., Smith, W. R. and Towns-Andrews, E. *Rev. Sci. Instrum.* 1995, **66**, 1311
18 Brandrup, J. and Immergut, E. H. (Eds.) 'Polymer Handbook', Wiley, New York, 1989
19 Welberry, T. R. *Rep. Prog. Phys.* 1985, **48**, 1543
20 Enting, I. G. *J. Phys. C* 1977, **10**, 1379
21 Gates, D. J. and Westcott, M. *Proc. R. Soc. Lond.* 1988, **A416**, 443